

Article

The Origin of the Yellow Luminescence Band in Be-Doped Bulk GaN

Michael A. Reshchikov ^{1,*}  and Michal Bockowski ² ¹ Department of Physics, Virginia Commonwealth University, Richmond, VA 23220, USA² Institute of High Pressure Physics, Polish Academy of Sciences, Sokolowska 29/37, 01-142 Warsaw, Poland; bocian@unipress.waw.pl

* Correspondence: mreshchi@vcu.edu; Tel.: +1-(804)-828-1613

Abstract: Photoluminescence (PL) from Be-doped bulk GaN crystals grown by the High Nitrogen Pressure Solution method was studied and compared with PL from GaN:Be layers on sapphire grown by molecular beam epitaxy and metalorganic chemical vapor deposition techniques. The yellow luminescence band in the latter is caused by the isolated Be_{Ga} acceptor (the YL_{Be} band), while the broad yellow band in bulk GaN:Be crystals is a superposition of the YL_{Be} band and another band, most likely the C_N-related YL1 band. The attribution of the yellow band in bulk GaN:Be crystals to the Be_{Ga}O_N complex (a deep donor) is questioned.

Keywords: photoluminescence; point defects; GaN; beryllium; yellow luminescence

1. Introduction

GaN with a bandgap of 3.50 eV attracts significant attention from researchers due to its applications in light-emitting and high-power devices [1–4]. Point defects that may detrimentally affect the devices' efficiency and longevity are still poorly understood. Photoluminescence (PL) is a powerful research tool that reveals the properties of point defects, such as charge state, transition levels, and carrier capture coefficients [5–7].

The most-studied defect-related PL band in GaN is the yellow luminescence (YL) band [8–10]. In undoped GaN grown by metalorganic chemical vapor deposition (MOCVD), the YL band with a maximum at 2.17 eV and zero-phonon line (ZPL) at 2.59 eV (labeled the YL1 band) is commonly observed due to contamination with carbon and attributed to the C_N acceptor [10–14]. The YL1 band can also be recognized in PL spectra from undoped GaN grown by other techniques such as the High Nitrogen Pressure Solution (HNPS) method [15] and the hydride vapor phase epitaxy (HVPE) method [12]. Very low concentrations of carbon (10¹⁵–10¹⁶ cm^{−3}) in HVPE-grown undoped GaN lead to the quantum efficiency of the YL1 band close to unity thanks to a relatively high hole-capture cross-section of the C_N defect [16,17]. This explains why the C_N-related YL1 band is omnipresent in undoped GaN and GaN doped with various impurities.

A different (as will be shown below) yellow band is observed in GaN doped or implanted with beryllium (Be) [9,17–19]. A renewed interest in doping III-nitrides with Be is fueled by recent findings that shallow Be-related acceptors can potentially be used for conductive *p*-type GaN and AlN [20–22]. We recently studied PL from more than 100 Be-doped GaN samples grown by MOCVD and molecular beam epitaxy (MBE), as well as GaN samples grown by HVPE and implanted with Be or co-implanted with Be and F [23,24]. In almost all these samples, the YL band is the dominant defect-related PL band with absolute internal quantum efficiency approaching unity in some samples. This YL band, with a maximum at 2.15 eV and specific properties (labeled the YL_{Be} band), is now reliably attributed to the isolated Be_{Ga} acceptor [25].

In fair agreement with the theoretical predictions of Lany and Zunger [26], deep and shallow states of the Be_{Ga} acceptor are found in PL experiments [25]. Two deep polaronic



Citation: Reshchikov, M.A.; Bockowski, M. The Origin of the Yellow Luminescence Band in Be-Doped Bulk GaN. *Solids* **2024**, *5*, 29–44. <https://doi.org/10.3390/solids5010003>

Academic Editor: Antonio Polimeni

Received: 19 November 2023

Revised: 29 December 2023

Accepted: 1 January 2024

Published: 4 January 2024



Copyright: © 2024 by the authors. Licensee MDPI, Basel, Switzerland. This article is an open access article distributed under the terms and conditions of the Creative Commons Attribution (CC BY) license (<https://creativecommons.org/licenses/by/4.0/>).

configurations with a hole localized at a neighboring N atom in the c direction and one of three other directions have $-/0$ transition levels at 0.38 ± 0.03 eV (configuration Be2) and 0.33 ± 0.05 eV (Be1), respectively, above the valence band maximum (VBM) in the limit of low temperatures. Electron transitions from the conduction band to these levels are responsible for the YL_{Be2} and YL_{Be1} components of the YL_{Be} band, respectively [25]. The shallow state with a delocalized hole (Be3) is at 0.24 ± 0.02 eV above the VBM. Electron transitions from the conduction band to the shallow level cause the ultraviolet luminescence (UVL) band, with the main peak at 3.26 eV (labeled the UVL_{Be3}). Although the UVL_{Be3} band resembles the Mg-related UVL band (the UVL_{Mg} band with the main peak at 3.28 eV), these two bands can be reliably distinguished thanks to their specific temperature dependences [25]. In particular, the ratio of intensities of the UVL_{Be3} and YL_{Be2} bands, $I_{Be3}^{UVL}/I_{Be2}^{YL}$, is the same for all GaN:Be samples, and it can be fitted with the following expression:

$$\frac{I_{Be3}^{UVL}}{I_{Be2}^{YL}} = \delta \exp\left(-\frac{\Delta E}{kT}\right), \quad (1)$$

where δ is approximately equal to the ratio of the electron-capture coefficients for the Be3 and Be2 states of the Be_{Ga} acceptor (18 ± 8) and ΔE is the energy difference between these states (140 ± 10 meV). This property allows us to reliably recognize PL from the Be_{Ga} acceptor in GaN:Be samples, even when other PL bands contribute to the PL spectrum.

Another unique feature of the YL_{Be} band (observed in all studied GaN:Be layers on sapphire) is two-step quenching and complete disappearance at temperatures close to room temperature. The first step at about 100 K is attributed to a replacement of the YL_{Be1} component by the YL_{Be2} component after a captured hole transits from Be1 to Be2 over a potential barrier. The second quenching begins at about 200 K. The activation energy of this quenching is 0.30 eV in n -type samples, which led us to erroneously assume that the quenching is caused by the thermal emission of holes from the deep polaronic state to the valence band [23]. However, a more detailed analysis indicated that the quenching is caused by the thermal emission of holes from the shallow Be_{Ga} state (Be3, at ~ 0.20 eV at these temperatures) to the valence band. The larger nominal activation energy and relatively high temperatures at which the quenching of PL from such a shallow level occurs are explained by the feeding mechanism [25]. Namely, holes from the deep polaronic state are excited to the shallow state before they escape to the valence band, so that the measured activation energy of the quenching is the sum of the shallow state energy (E_3) and the energy difference between the shallow and deep states (ΔE).

A similar and very bright YL band with a maximum at 2.1–2.2 eV is observed in bulk GaN:Be crystals produced by the HNPS growth method [27–29]. However, the properties of the YL band in these crystals (labeled YL_{bulk} , hereafter) appear to be different from those of the YL_{Be} band in GaN:Be layers grown by MBE or MOCVD. In particular, the YL_{bulk} band is strong at room temperature, and its quenching begins only at $T > 500$ K [28]. It can be excited resonantly, with photon energies down to ~ 2.7 eV [28,29]. These features of the YL_{bulk} band indicate that the related transition level is at least 0.8 eV above the VBM, much deeper than the levels of the YL_{Be} band. Teisseyre et al. [27] attributed the YL_{bulk} band to the $Be_{Ga}O_N$ complex (the YL_{BeO} , hereafter). The assignment is based on theoretical predictions [27] and seems reasonable because these samples contain very high concentrations of Be and O (about 10^{19} cm $^{-3}$). However, the $0/+$ transition level of the $Be_{Ga}O_N$ complex is calculated at 0.26 eV [27]. Moreover, first-principles calculations by another research group predict that the $Be_{Ga}O_N$ complex is electrically neutral and does not have transition levels in the band gap [23]. The controversy can be resolved if we assume that more than one PL band contributes to the broad YL_{bulk} band. Lamprecht et al. [28] proposed that the YL_{bulk} band consists of three components, with maxima at 1.88 eV (red band), 2.08, and 2.12 eV (yellow). The 2.08 eV component was attributed to the $Be_{Ga}O_N$ complex, while the 2.12 eV component was thought to be caused by the C_N acceptor. Time-resolved PL experiments using a shutter indicated that all three components decay very slowly, so the YL_{bulk} signal could be observed for several seconds [28].

In this work, we propose a solution to the problem of the yellow band in Be-doped GaN. The Be_{Ga}-related YL_{Be} band with its specific properties is found in bulk GaN crystals grown by the HNPS technique. It is buried under a stronger yellow band in bulk GaN:Be crystals (temporarily labeled YL_X). The YL_X band is caused by electron transitions from the conduction band (or from the shallow donors) to a deep level at 0.8–0.9 eV above the VBM and is likely the C_N-related YL1 band.

2. Materials and Methods

Be-doped GaN crystals were grown by the HNPS method at a growth temperature of 1450 °C and at 1 GPa of nitrogen pressure [30,31]. Beryllium doping was at a level of 10¹⁹ cm⁻³. The typical lateral size of spontaneously crystallized GaN:Be hexagonal platelets did not exceed 5 mm and the thickness was 150 μm. According to secondary ion mass spectrometry (SIMS) measurements performed at the Institute of Physics of the Polish Academy of Sciences with CAMECA IMS6F microanalyzer (Gennevilliers, France), GaN:Be crystals grown under similar conditions contain 3 × 10¹⁹ cm⁻³ of Be atoms, 2 × 10¹⁹ cm⁻³ of O, and 5 × 10¹⁷ cm⁻³ of C. The samples are semi-insulating. Point defects in similar crystals were previously studied by PL [27–29,31], positron annihilation [32], optically detected magnetic resonance (ODMR) [33], infrared absorption [34], and photo-induced electron paramagnetic resonance (photo-EPR) [35,36].

Steady-state PL was excited with a HeCd laser, dispersed by 1200 rules/mm grating in a 0.3 m monochromator, and detected by a cooled photomultiplier tube. Other details of PL experiments can be found elsewhere [7,13]. The as-measured PL spectra were corrected for the measurement system's spectral response, and PL intensity was additionally multiplied by λ³, where λ is the light wavelength, to present the PL spectra in units proportional to the number of emitted photons as a function of photon energy [13].

3. Results

3.1. PL Bands in Be-Doped GaN Grown by MOCVD and MBE Techniques

The shape and position of the YL_{Be} band are well reproduced in many GaN layers grown by MOCVD and MBE. Figure 1 shows representative PL spectra at *T* = 18 K. The shape of the YL_{Be} band can be fitted (the dashed line) with the following expression obtained in the one-dimensional configuration coordinate model [37]:

$$I^{PL}(\hbar\omega) = I^{PL}(\hbar\omega_{\max}) \exp \left[-2S_e \left(\sqrt{\frac{E_0^* - \hbar\omega + \Delta}{d_{FC}^g}} - 1 \right)^2 \right]. \quad (2)$$

Here, *S_e* is the Huang–Rhys factor in the excited state of the defect; *d_{FC}^g* = *E₀^{*}* − *ħω_{max}* is the Frank–Condon shift in the ground state; *E₀^{*}* = *E₀* + 0.5*ħΩ_e*, where *E₀* is the ZPL energy and *ħΩ_e* is the energy of the effective phonon mode in the excited state; and *ħω* and *ħω_{max}* are the photon energy and position of the PL band maximum, respectively. The Δ is a minor shift of the PL band maximum due to sample-dependent reasons such as in-plane biaxial strain in thin GaN layers grown on sapphire substrates (blue shift) or local electric fields (red shift).

In addition to the YL_{Be} band, PL spectra from Be-doped GaN grown by MOCVD and MBE contain two UVL bands: the Mg_{Ga}-related UVL_{Mg} band, with the first peak at 3.27 eV, and the Be-related UVL_{Be} band, with the first peak at 3.38 eV. Both peaks are followed by a few LO phonon replicas. The UVL_{Mg} band is caused by mild contamination with Mg during growth (especially significant in our MOCVD GaN:Be samples). The UVL_{Be} band was found in the majority of GaN:Be samples. In MBE-grown samples, it required activation by annealing at *T* > 750 °C (Figure 1). Our earlier attribution of this band to the shallow state of the Be_{Ga} acceptor [20] was later rejected, and the band is preliminary attributed to a complex defect involving Be [25].

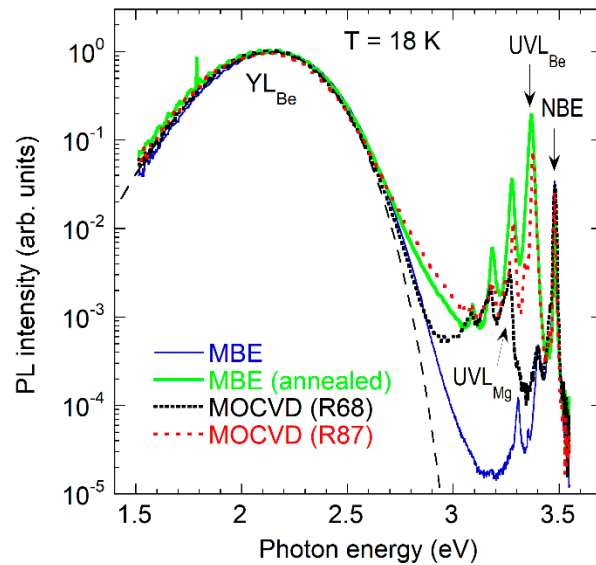


Figure 1. Normalized PL spectra at $T = 18$ K from MBE GaN:Be (sample 0408a, as grown and annealed at 800 °C) and two MOCVD GaN:Be (samples R68 and R87). The Be_{Ga} -related YL_{Be} band is very strong in all the samples (the quantum efficiency is close to unity). The dashed line is calculated using Equation (2) with the following parameters: $S_e = 22$, $E_0^* = 3.2$ eV, and $d_{\text{FC}}^{\text{S}} = 1.05$ eV. The UVL_{Be} band (presumably caused by a Be-containing complex) emerges in MBE GaN:Be samples only after thermal annealing. In MOCVD GaN:Be, the UVL_{Be} band is strong in some samples (such as R87) but could not be resolved in other samples (R68). The Mg_{Ga} -related UVL_{Mg} band is often observed in MOCVD GaN:Be samples because of contamination with Mg. NBE is the near-band-edge emission.

The best way to recognize the Be_{Ga} -related YL_{Be} band is to investigate the temperature evolution of the PL spectrum, the characteristic features of which were reproduced in all studied GaN:Be samples grown by MBE and MOCVD [25]. The YL_{Be} band is quenched in two steps. At $T \approx 100$ K, the YL_{Be} band intensity drops (usually by a factor of about 2) and the band abruptly redshifts by up to 50 meV. This behavior is explained by the relaxation of the bound hole from the polaronic state Be_1 at 0.33 eV to the polaronic state Be_2 at 0.38 eV. At $T > 180$ K, the second quenching is observed (Figure 2). In conductive n -type GaN:Be samples, the second quenching reveals an activation energy of 0.30 eV, while in semi-insulating samples, the quenching occurs by the abrupt and tunable quenching (ATQ) mechanism [38].

The most important feature of the temperature evolution of PL is the emergence of a UVL band (UVL_{Be_3}) at $T > 140$ K (Figure 2). The shift of the UVL maximum with temperature is shown in Figure 3. At $T < 25$ K, the UVL band is caused by donor-acceptor-pair (DAP)-type transitions of electrons from shallow O_{N} donors to shallow Mg_{Ga} acceptors. At $T > 50$ K, the DAP peaks are replaced with similar peaks caused by electron transitions from the conduction band to the Mg_{Ga} acceptors (eA transitions). At $T > 130$ K, the UVL_{Mg} band is quenched by the ATQ mechanism. A similar in shape but slightly red-shifted UVL_{Be_3} band emerges at higher temperatures. It can be seen from Figure 3 that the ZPL of the UVL_{Be_3} is red-shifted by 13 ± 3 meV from the ZPL of the UVL_{Mg} band. Since the transition level of the shallow Mg_{Ga} acceptor is located at 223 ± 3 meV above the VBM at $T = 18$ K [12], we conclude that the shallow $-/0$ transition level of the Be_{Ga} acceptor (the Be_3 state) is located at 236 ± 5 meV above the VBM. With increasing temperature, the Be_3 level moves towards the valence band (0.20 eV at $T \approx 200$ K) [25].

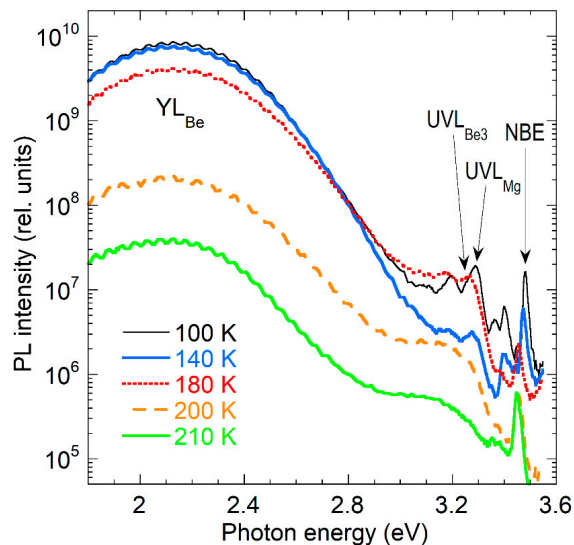


Figure 2. PL spectra from MOCVD GaN:Be sample R87 at selected temperatures and $P_{exc} = 0.005 \text{ W/cm}^2$. The Be_{Ga} -related YL_{Be} band is quenched by the ATQ mechanism at $T > 160 \text{ K}$. The Mg_{Ga} -related UVL_{Mg} band disappears at $T > 130 \text{ K}$ and is replaced with the Be_{Ga} -related UVL_{Be3} band emerging at higher temperatures.

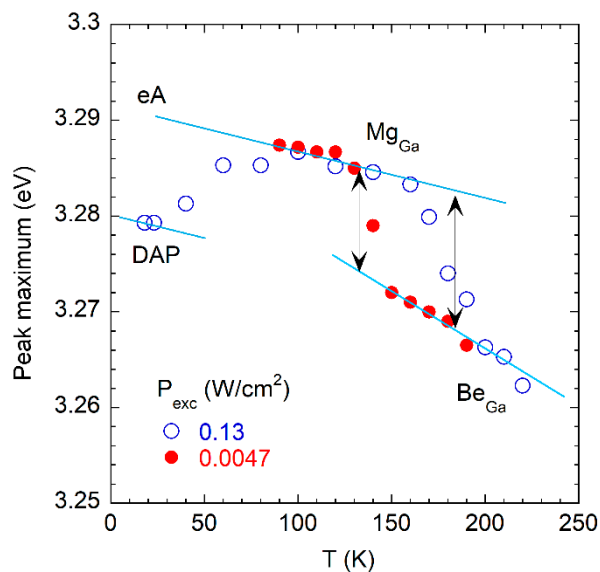


Figure 3. Dependence of UVL peak position on temperature for MOCVD GaN:Be (sample R134). The UVL_{Mg} band is quenched at $T \approx 130 \text{ K}$ ($P_{exc} = 0.0047 \text{ W/cm}^2$) and $T \approx 170 \text{ K}$ ($P_{exc} = 0.13 \text{ W/cm}^2$) by the ATQ mechanism. At these temperatures, the UVL_{Mg} band is replaced by the UVL_{Be3} band. The lengths of the arrows are 11 and 15 meV.

In agreement with the model proposed in Ref. [25], the ratio $\text{UVL}_{\text{Be3}}/\text{YL}_{\text{Be}}$ of PL intensities is the same in all GaN:Be samples. This ratio is described in a wide range of temperatures with Equation (1), where ΔE is the energy distance between the Be2 and Be3 states ($\Delta E = 140\text{--}145 \text{ meV}$). Figure 4 shows the dependence for two samples. In the MOCVD GaN:Be sample, the UVL_{Mg} band is quenched and replaced by the UVL_{Be3} band at $T > 140 \text{ K}$ (compare Figures 3 and 4 for this sample).

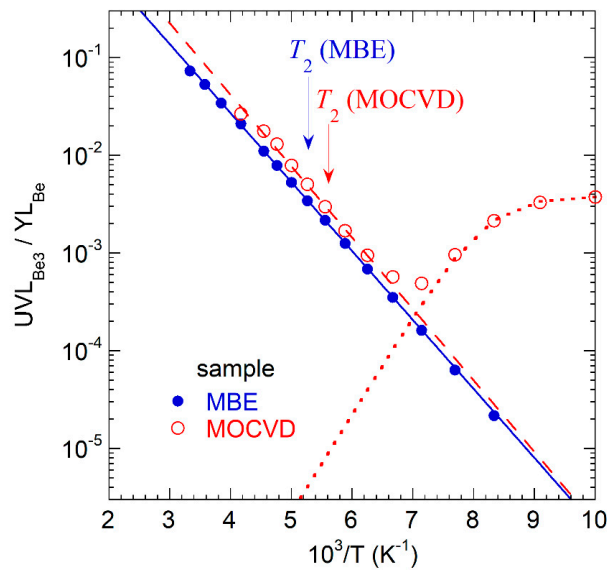


Figure 4. Temperature dependence of the integrated UVL_{Be3} and YL_{Be} band intensities ratio in selected GaN:Be samples (MBE 0020-1 and MOCVD R134) at $P_{exc} = 0.0047 \text{ W/cm}^2$. The lines are calculated using Equation (1) with the following parameters: $\Delta E = 140 \text{ meV}$, $\delta = 18$ (solid line), and $\Delta E = 145 \text{ meV}$, $\delta = 35$ (dashed line). The dotted line is calculated using Equation (4), with $C = 2 \times 10^8$ and $E_A = 200 \text{ meV}$. The arrows show the critical temperature of the YL_{Be} quenching.

A remarkable feature of this model is that the second step of the YL_{Be} quenching is caused by the thermal emission of holes, not from a deep but from the shallow Be3 level, to the valence band. In particular, the activation energy of 0.30 eV obtained from this quenching in conductive n -type GaN:Be samples is the sum of the Be3 ionization energy and ΔE [25]. From this, the deepest polaronic state of the Be_{Ga} acceptor is found at $0.38 \pm 0.03 \text{ eV}$ above the VBM in the limit of low temperatures ($\approx 0.30 \text{ eV}$ at $T = 200 \text{ K}$). The unique interplay of the UVL_{Be3} and YL_{Be} bands will be used below to recognize the YL_{Be} band in bulk GaN crystals.

3.2. The Yellow Band in Bulk GaN:Be Grown by High-Pressure Technique

Figure 5 shows PL spectra from bulk GaN:Be excited above-bandgap (with the 325 nm line of the HeCd laser at 3.81 eV) and below-bandgap (with the 442 nm line of the HeCd laser at 2.80 eV). The spectra are compared with the PL spectrum from MBE-grown GaN:Be. In the case of the usual above-bandgap excitation, a very weak near-band-edge (NBE) emission is detected at 3.47 eV. The UVL_{Mg} band appears as a structureless shoulder at about 3.2 eV. We assume that its ZPL and LO phonon replicas are unresolved because of strong local electric fields caused by short-range potential fluctuations in heavily doped and compensated GaN:Be [39].

The yellow band (YL_{bulk}) at $\sim 2.1 \text{ eV}$ is broad and very strong, in agreement with earlier reports [28,29]. With increasing excitation intensity, P_{exc} , from 10^{-5} to $\sim 100 \text{ W/cm}^2$, it blueshifts by about 0.1 eV. After a laser pulse at $T = 18 \text{ K}$, the PL intensity decays nonexponentially, approximately as $t^{-1.2}$ at time delays t between 1 and 1000 s, and the band redshifts by almost 0.1 eV. Such behavior agrees with the presence of potential fluctuations.

The yellow band in bulk GaN:Be crystals can also be excited below the bandgap. The spectrum obtained after excitation with the 442 nm line of the HeCd laser (2.8 eV) is shown in Figure 5 with filled circles. This band (temporarily labeled YL_X) is also broad and its maximum is at 2.07 eV. Interestingly, the sum of the YL_{Be} band in MBE GaN:Be and the YL_X band matches the shape of the YL_{bulk} band observed after the above-bandgap excitation (Figure 5). This is the first indication that the YL_{bulk} band may consist of two unresolved broad bands, one of which is the well-studied Be_{Ga} -related YL_{Be} band. A

stronger argument follows from the analysis of the evolution of the PL spectrum with temperature, as discussed below.

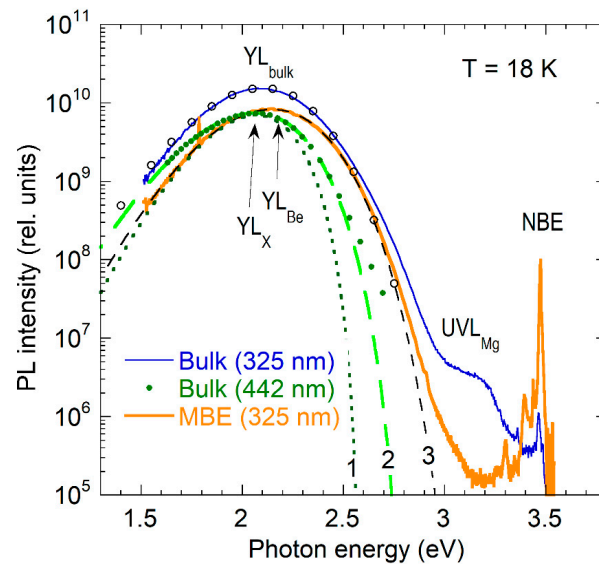


Figure 5. PL spectra at $T = 18$ K and $P_{exc} = 0.005$ W/cm² from bulk GaN:Be (excited with HeCd laser at 325 nm and 442 nm) and MBE GaN (sample 0408a, not annealed). The PL spectrum excited at 442 nm is arbitrarily shifted vertically. The dashed and dotted lines are calculated using Equation (2) with the following parameters: $S_e = 7.4$, $E_0^* = 2.67$ eV, and $d_{FC}^s = 0.50$ eV, $\Delta = -0.1$ eV (curve 1, the YL1 band); $S_e = 11$, $E_0^* = 2.8$ eV, and $d_{FC}^s = 0.74$ eV (curve 2, the YL_X band); and $S_e = 21$, $E_0^* = 3.2$ eV, and $d_{FC}^s = 1.05$ eV (curve 3, the YL_{Be} band). The empty circles are the sum of 2 and 3. The UVL_{Mg} band is caused by contamination with Mg.

Figure 6 shows the PL spectrum from bulk GaN:Be at selected temperatures. The intensity of the YL_{bulk} band changes insignificantly with increasing temperature from 18 to 320 K. The intensity of the UVL band decreases between 18 and 140 K and then increases (between 140 and 200 K). While the fine structure of the UVL band cannot be resolved, the increase in the UVL intensity is very similar to that observed in the GaN:Be samples grown by MBE and MOCVD [25].

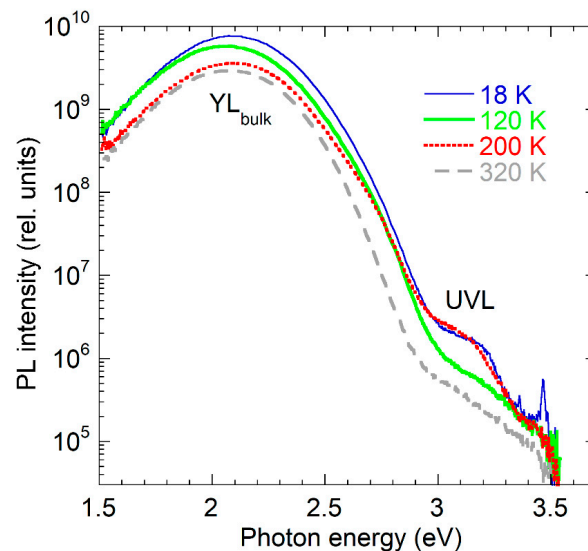


Figure 6. PL spectra from bulk GaN:Be at selected temperatures and $P_{exc} = 0.005$ W/cm². The YL_{bulk} band consists of unresolved YL_{Be} and YL_X bands. The Mg_{Ga}-related UVL_{Mg} band at 18 K is replaced by a similar Be_{Ga}-related UVL_{Be3} band at $T > 120$ K (both labeled UVL).

Figure 7 compares PL spectra at $T = 200$ K for bulk GaN:Be (at two crystal locations) and GaN:Be layers grown by MBE and MOCVD (arbitrarily shifted vertically to match the UVL intensity). The ratio of intensities UVL_{Be3}/YL_{Be} at the selected temperature must be the same in all Be-doped GaN samples. Assuming that the UVL_{Be3} band emerges with the temperature [25], we conclude that the YL_{Be} band in bulk GaN is hidden under a stronger yellow band of different origin (YL_X).

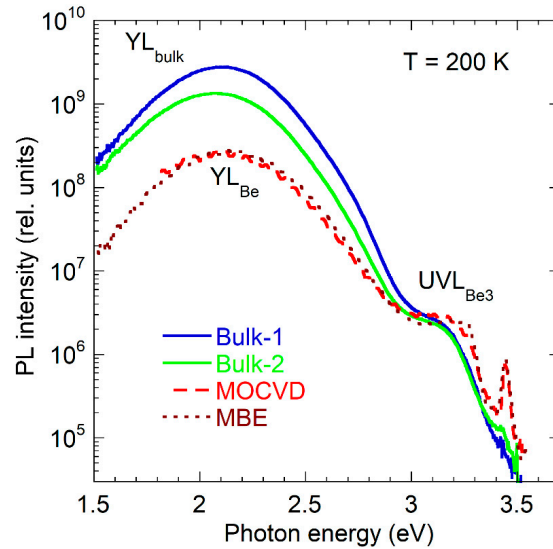


Figure 7. PL spectra at $T = 200$ K and $P_{exc} = 0.005$ W/cm² from bulk GaN:Be (in two locations of the sample) compared with the PL spectra from MOCVD GaN:Be (sample R26) and MBE GaN:Be (sample 0020-1). The spectra for the MBE and MOCVD samples are shifted vertically to match the intensity of the UVL_{Be3} band in all three samples.

Figure 8 shows an Arrhenius plot for the studied PL bands in bulk GaN:Be. The expected temperature dependence of the Mg_{Ga} -related UVL_{Mg} intensity is shown with a dotted line. The temperature dependences for the Be_{Ga} -related YL_{Be} band (shown with dashed lines) are simulated to fit the UVL_{Be3} dependences by fixing the UVL_{Be3}/YL_{Be} ratio according to Equation (1) with earlier-found parameters.

The first step of the YL_{Be} quenching is expected at $T \approx 100$ K but cannot be resolved. The YL_{Be} band hides under a stronger yellow band at $T < 200$ K and completely disappears at temperatures approaching room temperature, as expected [25]. We estimate that the YL_X band is stronger than the YL_{Be} band by a factor of 2–5 at $T < 200$ K.

We also studied the temperature dependence of the YL_{bulk} full width at half maximum (FWHM or W) and compared it with that for the YL_{Be} band in the GaN:Be samples grown by MOCVD (Figure 9). For PL bands that are broad due to strong electron–phonon coupling, the $W(T)$ dependence can be fitted with the following expression [6]:

$$W(T) = W(0) \sqrt{\coth\left(\frac{\hbar\Omega_e}{2kT}\right)}, \quad (3)$$

where $\hbar\Omega_e$ is the energy of the effective phonon mode. For MOCVD-grown GaN:Be samples, the fit with $\hbar\Omega_e = 38$ meV is relatively good, and the value of the single fitting parameter is typical for defects in GaN (between 23 and 56 meV) [37,40,41]. However, the $W(T)$ dependence for the YL_{bulk} band in bulk GaN:Mg shows abnormal narrowing with increasing temperature from ~ 170 to 250 K. This temperature region roughly corresponds to the region where the YL_{Be} band is quenched. We conclude that at $T > 250$ K, the contribution of the YL_{Be} band to the YL_{bulk} band can be ignored and only the YL_X band remains. The FWHM of the YL_X band is smaller than that of the YL_{Be} band, while the parameter $\hbar\Omega_e$ is larger (Figure 9).

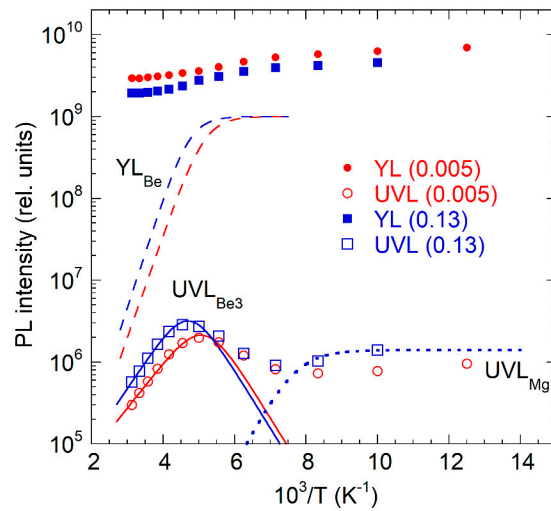


Figure 8. Temperature dependences of PL intensities at $P_{exc} = 0.005$ and 0.13 W/cm² from bulk GaN:Be (divided by P_{exc} for convenience of comparison). The dashed lines show the expected dependences of the YL_{Be} component of the YL band. The solid lines are expected dependences of the UVL_{Be3} band. The UVL_{Be3}/YL_{Be} ratios are described by Equation (1), in which $E_A = 140$ meV and $\delta = 18$ ($P_{exc} = 0.005$) and $\delta = 13.5$ ($P_{exc} = 0.13$). The dotted line shows the expected dependence for the UVL_{Mg} band described by Equation (4), with $E_A = 170$ meV and $C = 3.5 \times 10^6$.

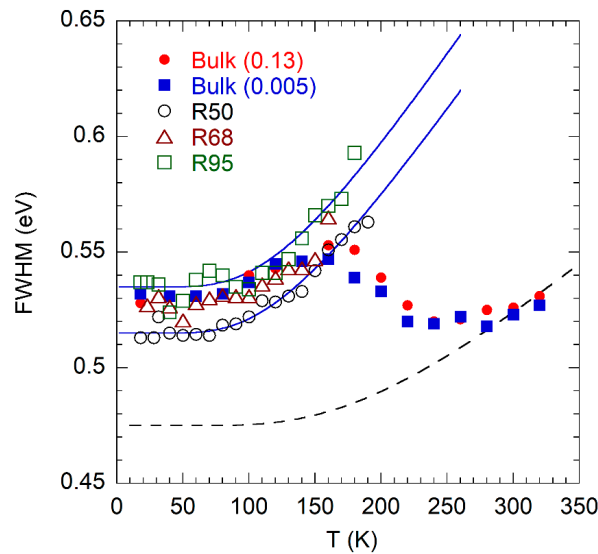


Figure 9. Temperature dependence of the FWHM of the YL_{bulk} band in bulk GaN:Be for $P_{exc} = 0.005$ and 0.13 W/cm² (solid symbols) and the YL_{Be} band in three MOCVD GaN:Be samples (empty symbols). The dependences for the MOCVD samples are fitted using Equation (3), with $\hbar\Omega_e = 38$ meV (solid lines). The dashed line, obtained using Equation (3) with $W(0) = 0.475$ eV and $\hbar\Omega_e = 60$ meV, illustrates a possible dependence for the YL_X component of the YL_{bulk} band.

Figure 10 shows the temperature dependence of the YL_{bulk} band maximum (shifted up by 23 meV for $P_{exc} = 0.005$ W/cm²) in comparison with the dependence for the YL_{Be} band in the MOCVD and MBE GaN:Be samples. The sudden shift at about 100 K is similar in all the samples, and it can be explained by replacing the YL_{Be1} with the YL_{Be2} , PL bands associated with two deep polaronic states of the Be_{Ga} acceptor [25]. At $T > 230$ K, the band maximum corresponds to the YL_X band because the YL_{Be} band is quenched. Note that the YL_{bulk} band shifts significantly with excitation intensity (up to 0.1 eV with a variation of P_{exc} from 10^{-5} to ~ 100 W/cm²), whereas the shift of the YL_{Be} band in the MOCVD and MBE GaN:Be samples is insignificant.

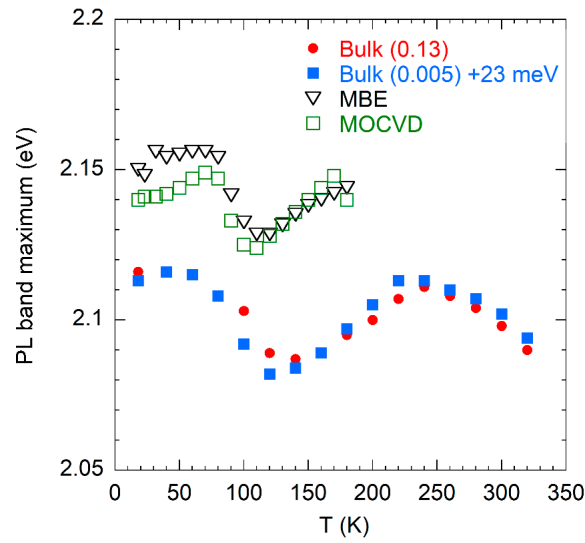


Figure 10. Temperature dependence of the YL_{bulk} band maximum in bulk GaN:Be for $P_{\text{exc}} = 0.005 \text{ W/cm}^2$ (blue-shifted by 23 meV for convenience of comparison) and 0.13 W/cm^2 (solid symbols) and the YL_{Be} band in the MOCVD and MBE GaN:Be samples at $P_{\text{exc}} = 0.005 \text{ W/cm}^2$ (empty symbols).

To further explore the properties of the YL_X band, we conducted PL experiments by using a high-temperature cryostat (Figure 11). The YL_X band is quenched by the ATQ mechanism, which is typical for defects in semi-insulating GaN [38]. Formally, it can be described with the commonly used expression:

$$I^{PL}(T) = \frac{I^{PL}(0)}{1 + C \exp\left(\frac{-E_A}{kT}\right)} \quad (4)$$

However, unlike the PL quenching in conductive n -type GaN, the parameter E_A does not have a physical meaning [17]. The quenching is very abrupt, yet the slope of the quenching could be smoothed by potential fluctuations [42], or other reasons [38]. The quenching is tunable by excitation intensity.

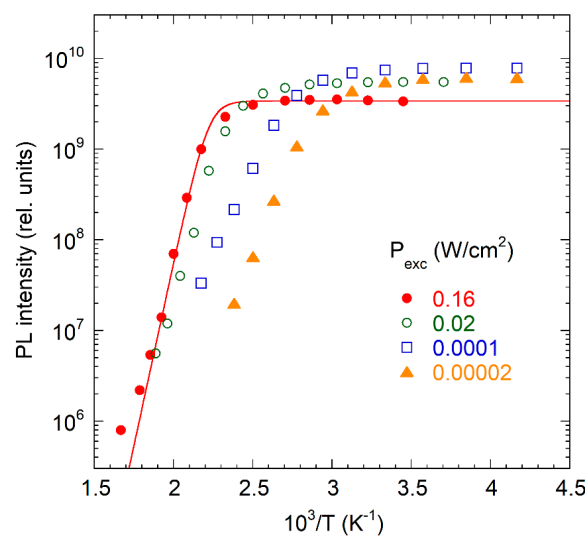


Figure 11. Abrupt and tunable quenching of the YL_{bulk} band in bulk GaN:Be. The PL intensity is divided by P_{exc} for convenience of comparison. The solid curve is calculated using Equation (4), with $C = 8 \times 10^{17}$ and $E_A = 1.6 \text{ eV}$.

4. Discussion

The results of this study indicate that at least two PL bands contribute to the YL_{bulk} band, with a maximum at about 2.1 eV in bulk GaN:Be grown by the HNPS method. These are the YL_{Be} band (with a maximum at 2.15 eV) associated with the isolated Be_{Ga} acceptor and the YL_X band (at ~ 2.06 eV) caused by a different defect. Since the YL_{Be} band is well studied [25], we will focus below on the analysis of the YL_X band, which is the strongest PL band at all studied temperatures.

4.1. Type of Transition

The YL_X band at $T = 18$ K can be excited below-bandgap, with photon energies of 2.8 eV (Figure 5). Earlier, the onset of the PL excitation (PLE) spectrum of the yellow band was found at 2.8 eV at 7 K, and the YL_{bulk} band could be excited with a 2.78 eV laser [28]. At room temperature (when we expect only the YL_X band), the PLE spectrum also shows an onset at about 2.7–2.8 eV [29]. We assume that the YL_X band is caused by electron transitions from the conduction band (or from shallow donors) to a deep defect level, as it occurs for almost all defects in GaN [7,17]. Then, the results of the current work and those of previous studies indicate that the related defect level is located no closer than 0.8 eV to the VBM. Nonexponential and slow PL decay after a laser pulse agrees with the assumed type of transition. This PL cannot be caused by transitions from an excited state to the ground state of some defect because such transitions are characterized by exponential PL decay, even at very low temperatures, and positions of such PL bands are not affected by local electric fields [7,17]. At this point, transitions from a deep donor to an acceptor (or a deeper donor) cannot be excluded since such transitions are possible in heavily doped GaN and are characterized by slow, nonexponential decay. If this was the case, the defect level responsible for the YL_X band would be much closer to the VBM than 0.8 eV. However, the quenching of the YL_X band at $T > 450$ K (Figure 11 and the data in Ref. [28]) favors the assumption that the related defect level is at 0.8–0.9 eV above the VBM. It was shown in Ref. [17] that for defects with relatively strong PL in GaN, the quenching begins at $T = 400$ – 500 K (at $P_{\text{exc}} \approx 0.1$ W/cm² when the quenching occurs by the ATQ mechanism) if the defect level is located at 0.6–1.0 eV above the VBM. Transitions from the conduction band (or from shallow donors) to a defect level at ~ 0.8 eV above the VBM may be characterized by a nonexponential, slow decay of PL and by relatively large PL band shifts with a variation of P_{exc} if local electric fields (e.g., due to potential fluctuations) are present. ODMR and photo-EPR studies of the yellow band in similar bulk GaN:Be crystals support this type of transition [33,35]. We exclude the possibility of electron transitions from a defect level located in the upper part of the gap to the valence band as the origin of the YL_X band. Such transitions cannot be observed because photogenerated holes are captured by various acceptors with the multiphonon nonradiative mechanism many orders of magnitude faster than via radiative transitions [7].

4.2. On Identification of the YL_X Band in Bulk GaN

The observed broad YL_{bulk} band in bulk GaN:Be consists of at least two unresolved bands, one of which is a well-studied YL_{Be} band associated with the isolated Be_{Ga} acceptor. Another PL band (temporarily labeled YL_X) is caused by electron transitions from the conduction band (or shallow donors) to a deep defect (donor or acceptor), with a transition level at 0.8–0.9 eV above the VBM. Since the main difference between GaN:Be layers grown by MBE or MOCVD methods and bulk GaN:Be crystals grown by the HNPS method is a high concentration of oxygen in the latter, it is tempting to attribute it to the $\text{Be}_{\text{Ga}}\text{O}_{\text{N}}$ complex, which is expected to be a deep donor [27]. However, the first-principles calculations using the Heyd–Scuseria–Ernzerhof (HSE) hybrid functional [43] predict that the 0/+ level of the $\text{Be}_{\text{Ga}}\text{O}_{\text{N}}$ defect is located at 0.26 eV above the VBM [27], or that this defect has no transition levels in the bandgap [23]. Whereas fair agreement of theoretical predictions with experimental findings is observed for the Be_{Ga} acceptor, the disagreement for the 0/+ level of the $\text{Be}_{\text{Ga}}\text{O}_{\text{N}}$ defect is significant (Table 1).

Table 1. Calculated and experimentally found values (all in eV) of the charge transition levels relative to the VBM and PL band maxima (for $E_g = 3.50$ eV) for defects that may contribute to the YL_{bulk} band in Be-doped GaN, assuming that the YL_X band is caused by the $Be_{Ga}O_N$ complex.

Source	$Be_{Ga} (-/0)$		$Be_{Ga}O_N (0/+)$		$C_N (-/0)$		References		
	Deep	Shallow	Deep	Deep	Deep				
	E_A	$\hbar\omega_{\text{max}}$	E_A	$\hbar\omega_{\text{max}}$	E_A	$\hbar\omega_{\text{max}}$			
VDW ¹	0.55	1.80			0.26	2.08	0.90	2.14	[11,27,44]
DD ²	0.58	1.72	0.24	3.20	–	–	0.93	2.08	[13,20,23]
SHW ³	0.65	1.67							[45]
LZ ⁴	0.45	2.02	0.15	~3.3					[26]
Experiment	0.33 0.38	2.15	0.236	3.26	0.8–0.9	2.06	0.916	2.17	[12,25] and this work

¹ Van de Walle's group. ² D. Demchenko. ³ Su-Huai Wei. ⁴ Lany and Zunger.

Another possibility is that the YL_X band is the C_N -related $YL1$ band slightly broadened and redshifted because of potential fluctuations (Figure 12). Both PL bands are quenched at $T > 500$ K in semi-insulating GaN (at $P_{\text{exc}} \approx 0.1$ W/cm²). The concentration of carbon impurities in the studied bulk GaN:Be samples is about 5×10^{17} cm⁻³, which is enough to cause a strong yellow band.

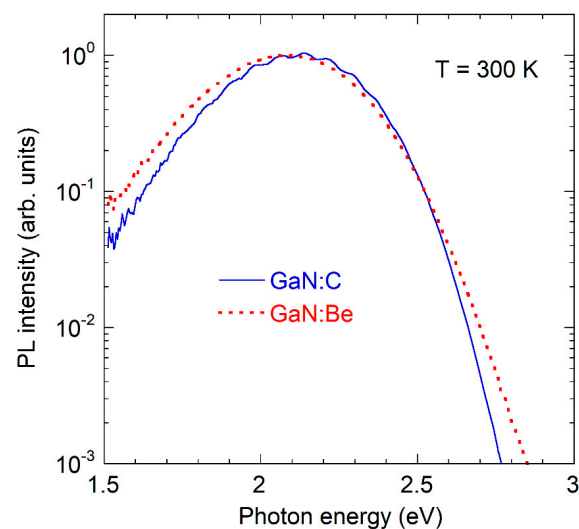


Figure 12. Comparison of the YL_X band in bulk GaN:Be with the $YL1$ band in MOCVD GaN:C at $T = 300$ K.

Below, we will discuss two candidates for the YL_X band (C_N acceptor and $Be_{Ga}O_N$ donor). Parameters of defects that may contribute to the YL_{bulk} band are given in Table 2. The hole-capture coefficient, C_p , for the C_N acceptor is $(3.7 \pm 1.6) \times 10^{-7}$ cm³/s. The C_p for the Be_{Ga} acceptor was estimated from the YL_{Be} quenching as 4×10^{-7} cm³/s. However, careful analysis of PL quenching in numerous MOCVD GaN:Be samples (which contain C and Be, with concentrations of about 10^{17} cm⁻³ and $(1-30) \times 10^{17}$ cm⁻³, respectively) shows that the C_p for the Be_{Ga} acceptor is larger, which is consistent with the capture of holes by a shallow acceptor level located at 0.2 eV above the VBM. It was shown in Ref. [25] that $C_p = 10^{-6}$ cm³/s agrees with the experimental data. Note that for another shallow acceptor (Mg_{Ga}), C_p is also 10^{-6} cm³/s. We will consider this value hereafter for the Be_{Ga} acceptor that captures holes at its shallow level at 0.2 eV above the VBM [25]. The C_p for the $Be_{Ga}O_N$ complex is expected to be significantly smaller because of the donor nature of this defect. The C_p for donors in GaN varies from 10^{-10} to 4×10^{-8} cm³/s [17]. At low enough temperatures (before the PL quenching begins), the PL intensity from defects in GaN (both conductive n -type and semi-insulating) is proportional to the concentration of defects and

their hole-capture coefficient, i.e., $I_i^{PL} = AC_{pi}N_i$ for defect i , where A is a constant. From the experiment, $I_X^{PL}/I_{Be}^{PL} = 2-5$.

Table 2. Possible parameters of main defects in bulk GaN:Be.

Scenario	Concentration of Defects (cm ⁻³)				Hole-Capture Coefficient (cm ³ /s)		
	Be _{Ga}	Be _{Ga} O _N	O _N	C _N	Be _{Ga}	Be _{Ga} O _N	C _N
1 (X = C _N)	10 ¹⁷	3 × 10 ¹⁹	10 ¹⁷	10 ¹⁸	10 ⁻⁶	10 ⁻⁹	4 × 10 ⁻⁷
2 (X = Be _{Ga} O _N)	10 ¹⁸	3 × 10 ¹⁹	10 ¹⁸	10 ¹⁸	10 ⁻⁶	10 ⁻⁷	4 × 10 ⁻⁷

4.2.1. Can the YL_X Band Be the C_N-Related YL1 Band?

In the first scenario, the intensity of the YL1 band at $T \approx 100$ K is about 2–5 times higher than that of the YL_{Be} band, and the contribution of PL from the Be_{Ga}O_N complex is negligible. For this, the concentration of isolated Be_{Ga} defects should be about 10¹⁷ cm⁻³. Then, $I_C^{PL}/I_{Be}^{PL} = C_{p,C}N_C/C_{p,Be}N_{Be} = 4$ if we use the corresponding parameters in Table 2. Such a low concentration of isolated Be_{Ga} defects (by a factor of 30 lower than the total concentration of Be atoms) implies that the concentration of Be_{Ga}O_N complexes may reach 3 × 10¹⁹ cm⁻³, i.e., the majority of Be atoms form complexes with oxygen. The concentration of O_N donors may not exceed the total concentration of acceptors (C_N and Be_{Ga}) because the samples are semi-insulating and the Be_{Ga}O_N donors are neutral. Such a high concentration of Be_{Ga}O_N would not contribute to PL if the hole-capture coefficient for this donor is low ($I_{BeO}^{PL}/I_{Be}^{PL} = C_{p,BeO}N_{BeO}/C_{p,Be}N_{Be} = 0.3$ if C_p for the Be_{Ga}O_N complex is 10⁻⁹ cm³/s) or if the Be_{Ga}O_N is not participating in electron–hole recombination as it was predicted in Ref. [23].

4.2.2. Can the YL_X Band Be Caused by the Be_{Ga}O_N Complex?

In the second scenario, the intensity of the assumed YL_{BeO} band from the Be_{Ga}O_N complex at $T \approx 100$ K is about 2–5 times higher than that of the YL_{Be} band, and the YL1 band from the C_N acceptors is negligibly weak. For this, the concentration of isolated Be_{Ga} defects should be at least 10¹⁸ cm⁻³ (so that $I_C^{PL}/I_{Be}^{PL} = C_{p,C}N_C/C_{p,Be}N_{Be} < 0.4$), and the C_p for the Be_{Ga}O_N donor should be relatively high (so that $I_{BeO}^{PL}/I_{Be}^{PL} = C_{p,BeO}N_{BeO}/C_{p,Be}N_{Be} = 2-5$). This scenario would work if $N_{BeO} = 3 \times 10^{19}$ cm⁻³ and $C_{p,BeO} = 10^{-7}$ cm³/s (Table 2). The main argument against this scenario is a conflict between the predicted ionization energy of the Be_{Ga}O_N (0.26 eV or no level) [23,27] and the experimentally found transition level at 0.8–0.9 eV. However, a strong argument favoring this scenario was a good agreement between theoretical predictions and experiments in PL under hydrostatic pressure [27]. Below, we will suggest an alternative interpretation of these experiments.

4.3. Interpretation of Other Experiments

Exciting results were obtained in Ref. [27], where PL from bulk GaN:Be was studied at $T = 10$ K under hydrostatic pressure, p , up to 12.5 GPa. With increasing p , the YL band splits into two components: component A blue-shifts with a moderate rate (20 meV/GPa, similar to the typical shift of the C_N-related YL1 band), while component B blue-shifts much faster (about 90 meV/GPa). Component A was attributed to the C_N acceptor, while components B and C were related to the deep (polaronic) and shallow (delocalized) states of the Be_{Ga}O_N complex. A remarkable result is that at $p > 8$ GPa, component C emerges at about 3.6 eV and becomes the strongest PL band at $p > 9$ GPa. This unusual phenomenon was explained by the dual nature of the Be_{Ga}O_N defect: namely, the deeper state with a highly localized hole (calculated 0/+ level at 0.26 eV above the VBM at $p = 0$) moves towards the VBM with hydrostatic pressure. At $p = 8$ GPa, a shallow state of this defect (the 0/+ level at 0.12 eV above the VBM) with a delocalized hole becomes the most stable configuration. At pressures between 9 and 12.5 GPa, both PL signals are observed: a relatively narrow PL band close to the bandgap, which is caused by electron transitions

from the conduction band to the shallow level, and a broad band at about 3 eV, which is caused by electron transitions from the conduction band to the deep state of the $\text{Be}_{\text{Ga}}\text{O}_{\text{N}}$ defect. The calculated barrier between the shallow and deep states is 0.24 eV [27]. The same calculations predict that the polaronic state of the isolated Be_{Ga} defect is deeper (0.55 eV above the VBM), and the deep states of the Be_{Ga} and $\text{Be}_{\text{Ga}}\text{O}_{\text{N}}$ defects shift similarly with hydrostatic pressure [27].

We agree that component A of the yellow band can be the YL1 band caused by the C_{N} acceptor but suggest that component B is caused by the isolated Be_{Ga} defect (the $-/0$ transition level at 0.38 eV above the VBM and the PL band maximum at 2.15 eV). With increasing p , this level shifts towards the valence band and, at $p \approx 8$ GPa, intersects the shallow level of the Be_{Ga} (at 0.24 eV above the VBM at $p = 0$). At higher pressures, the UVL_{Be_3} band of the Be_{Ga} acceptor emerges even at $T = 10$ K because this configuration becomes the most stable. It may be interesting to test the above explanation by investigating MOCVD GaN:Be samples under hydrostatic pressure. As for the $\text{Be}_{\text{Ga}}\text{O}_{\text{N}}$ complexes, we expect that they are either nonradiative, weakly radiative, or “inert” defects, so that their contribution to PL can be ignored even if their concentration is about $3 \times 10^{19} \text{ cm}^{-3}$.

Our interpretation of the PL results is consistent with the results of photo-EPR studies on similar bulk Be-doped GaN crystals [35,36]. Willoughby et al. [35] initially attributed the photo-EPR signal from Be-doped GaN crystals to a Be-related acceptor, with the $-/0$ transition level at 0.7 eV above the VBM. However, these authors later revised their attribution and explained this photo-EPR signal by recombination of electrons with holes bound to the C_{N} acceptor [36]. Note that slow transients of the photo-EPR signal, explained by trapping electrons by a Be-related defect level close to the conduction band [36], could be caused by potential fluctuations and local electric fields. This is also consistent with the very slow PL decays for the YL_{bulk} band [28]. The attribution of the YL_{bulk} band to a superposition of the YL_{Be} and YL1 bands may also explain the results obtained by Glaser et al. [33]. They observed ODMR signals from bulk GaN:Be crystals grown by the HNPS method (with a carbon concentration of 10^{17} cm^{-3}) and noted that the g -values for the yellow band in these samples were very close to those for the YL band in undoped GaN (i.e., for the C_{N} -related YL1 band).

5. Conclusions

The broad yellow luminescence band in bulk GaN crystals grown by high-pressure technique and doped with Be consists of two unresolved bands: the Be_{Ga} -related YL_{Be} band and the YL_{X} band, which is most likely the C_{N} -related YL1 band. At $T > 200$ K, the YL_{Be} band is quenched, while the quenching of the YL_{X} band begins only at 400–500 K. We conclude that the yellow band, previously attributed to the $\text{Be}_{\text{Ga}}\text{O}_{\text{N}}$ complex based on first-principles calculations and PL experiments with hydrostatic pressure [27], is in fact the Be_{Ga} -related YL_{Be} band, whereas the $\text{Be}_{\text{Ga}}\text{O}_{\text{N}}$ defect is either optically inactive or its contribution to PL is negligible. At the same time, the concentration of the $\text{Be}_{\text{Ga}}\text{O}_{\text{N}}$ complexes in these bulk GaN crystals significantly exceeds the concentration of the isolated Be_{Ga} defects.

Author Contributions: Conceptualization, M.A.R. and M.B.; methodology, M.A.R. and M.B.; software, M.A.R.; validation, M.A.R. and M.B.; formal analysis, M.A.R.; investigation, M.A.R. and M.B.; resources, M.A.R. and M.B.; data curation, M.A.R.; writing—original draft preparation, M.A.R.; writing—review and editing, M.A.R. and M.B.; visualization, M.A.R.; supervision, M.A.R.; project administration, M.A.R.; funding acquisition, M.A.R. and M.B. All authors have read and agreed to the published version of the manuscript.

Funding: This research at VCU was funded by the National Science Foundation, grant number DMR-1904861. The work at IHPP was supported by the Polish National Centre for Research and Development through project TECHMATSTRATEG-III/0003/2019-00.

Data Availability Statement: Data are contained within the article.

Conflicts of Interest: The authors declare no conflict of interest.

References

1. Morkoç, H. *Handbook of Nitride Semiconductors and Devices*; Wiley: New York, NY, USA, 2008.
2. Pearton, S.J.; Zolper, J.C.; Shul, R.J.; Ren, F. GaN: Processing, defects, and devices. *J. Appl. Phys.* **1999**, *86*, 1–78. [[CrossRef](#)]
3. Li, G.; Wang, W.; Yang, W.; Lin, Y.; Wang, H.; Lin, Z.; Zhou, S. GaN-based light-emitting diodes on various substrates: A critical review. *Rep. Prog. Phys.* **2016**, *79*, 056501. [[CrossRef](#)] [[PubMed](#)]
4. Jones, E.A.; Wang, F.; Costinett, D. Review of Commercial GaN Power Devices and GaN-Based Converter Design Challenges. *IEEE J. Emerg. Sel. Top. Electron.* **2016**, *4*, 707–719. [[CrossRef](#)]
5. Dean, P.J. Photoluminescence as a diagnostic of semiconductors. *Prog. Cryst. Growth Charact.* **1982**, *5*, 89–174. [[CrossRef](#)]
6. Reshchikov, M.A.; Morkoç, H. Luminescence properties of defects in GaN. *J. Appl. Phys.* **2005**, *97*, 061301. [[CrossRef](#)]
7. Reshchikov, M.A. Measurement and analysis of photoluminescence in GaN. *J. Appl. Phys.* **2021**, *129*, 121101. [[CrossRef](#)]
8. Ogino, T.; Aoki, M. Mechanism of Yellow Luminescence in GaN. *Jpn. J. Appl. Phys.* **1980**, *19*, 2395–2405. [[CrossRef](#)]
9. Pankove, J.I.; Hutchby, J.A. Photoluminescence of ion-implanted GaN. *J. Appl. Phys.* **1976**, *47*, 5387–5390. [[CrossRef](#)]
10. Reshchikov, M.A. On the Origin of the Yellow Luminescence Band in GaN. *Phys. Stat. Sol. (b)* **2023**, *260*, 2200488. [[CrossRef](#)]
11. Lyons, J.L.; Janotti, A.; Van de Walle, C.G. Carbon impurities and the yellow luminescence in GaN. *J. Appl. Phys.* **2010**, *97*, 152108. [[CrossRef](#)]
12. Reshchikov, M.A.; McNamara, J.D.; Zhang, F.; Monavarian, M.; Usikov, A.; Helava, H.; Makarov, Y.; Morkoç, H. Zero-phonon line and fine structure of the yellow luminescence band in GaN. *Phys. Rev. B* **2016**, *94*, 035201. [[CrossRef](#)]
13. Reshchikov, M.A.; Vorobiov, M.; Demchenko, D.O.; Özgür, Ü.; Morkoç, H.; Lesnik, A.; Hoffmann, M.P.; Hörich, F.; Dadgar, A.; Strittmatter, A. Two charge states of the C_N acceptor in GaN: Evidence from photoluminescence. *Phys. Rev. B* **2018**, *98*, 125207. [[CrossRef](#)]
14. Zimmermann, F.; Beyer, J.; Röder, C.; Beyer, C.; Richter, E.; Irmscher, K.; Heitmann, J. Current Status of Carbon-Related Defect Luminescence in GaN. *Phys. Stat. Sol. (a)* **2021**, *218*, 2100235. [[CrossRef](#)]
15. Suski, T.; Perlin, P.; Teisseyre, H.; Leszczynski, M.; Grzegory, I.; Jun, J.; Boćkowski, M.; Porowski, S. Mechanism of yellow luminescence in GaN. *Appl. Phys. Lett.* **1995**, *67*, 2188–2190. [[CrossRef](#)]
16. Reshchikov, M.A.; Usikov, A.; Helava, H.; Makarov, Y.; Prozheeva, V.; Makkonen, I.; Tuomisto, F.; Leach, J.H.; Udwyary, K. Evaluation of the concentration of point defects in GaN. *Sci. Rep.* **2017**, *7*, 9297. [[CrossRef](#)] [[PubMed](#)]
17. Reshchikov, M.A. Photoluminescence from defects in GaN. In *Proceedings of SPIE 12421, Gallium Nitride Materials and Devices XVIII*; Fujioka, H., Morkoç, H., Schwarz, U., Eds.; SPIE: San Francisco, CA, USA, 2023; p. 1242109.
18. Ilegems, M.; Dingle, R. Luminescence of Be- and Mg-doped GaN. *J. Appl. Phys.* **1973**, *44*, 4234–4235. [[CrossRef](#)]
19. Chen, L.; Skromme, B. Spectroscopic Characterization of Ion-Implanted GaN. In *GaN and Related Alloys—2002*; Materials Research Society Symposium—Proceedings; Wetzel, C., Yu, E.T., Speck, J.S., Rizzi, A., Arakawa, Y., Eds.; Cambridge University Press: Boston, MA, USA, 2003; Volume 743, pp. 755–760.
20. Demchenko, D.O.; Vorobiov, M.; Andrieiev, O.; Myers, T.H.; Reshchikov, M.A. Shallow and deep states of beryllium acceptor in GaN: Why photoluminescence experiments do not reveal small polarons for defects in semiconductors. *Phys. Rev. Lett.* **2021**, *126*, 027401. [[CrossRef](#)]
21. Ahmad, H.; Lindemuth, J.; Engel, Z.; Matthews, C.M.; McCrone, T.M.; Doolittle, W.A. Substantial P-Type Conductivity of AlN Achieved via Beryllium Doping. *Adv. Mater.* **2021**, *33*, 2104497. [[CrossRef](#)]
22. Doolittle, W.A.; Matthews, C.M.; Ahmad, H.; Lee, S.; Ghosh, A.; Marshall, E.N.; Tang, A.L.; Manocha, P.; Yoder, D. Prospectives for AlN electronics and optoelectronics and the important role of alternative synthesis. *Appl. Phys. Lett.* **2023**, *123*, 070501. [[CrossRef](#)]
23. Vorobiov, M.; Andrieiev, O.; Demchenko, D.O.; Reshchikov, M.A. Point Defects in Beryllium Doped GaN. *Phys. Rev. B* **2021**, *104*, 245203. [[CrossRef](#)]
24. Reshchikov, M.A.; Andrieiev, O.; Vorobiov, M.; Demchenko, D.O.; McEwen, B.; Shahedipour-Sandvik, F. Photoluminescence from GaN implanted with Be and F. *Phys. Stat. Sol. (b)* **2023**, *260*, 2300131. [[CrossRef](#)]
25. Reshchikov, M.A.; Vorobiov, M.; Andrieiev, O.; Demchenko, D.O.; McEwen, B.; Shahedipour-Sandvik, F. Dual Nature of the Be_{Ga} Acceptor in GaN: Evidence from Photoluminescence. *Phys. Rev. B* **2023**, *108*, 075202. [[CrossRef](#)]
26. Lany, S.; Zunger, A. Dual nature of acceptors in GaN and ZnO: The curious case of the shallow Mg_{Ga} deep state. *Appl. Phys. Lett.* **2010**, *96*, 142114. [[CrossRef](#)]
27. Teisseyre, H.; Lyons, J.L.; Kaminska, A.; Jankowski, D.; Jarosz, D.; Boćkowski, M.; Suchocki, A.; Van de Walle, C.G. Identification of yellow luminescence centers in Be-doped GaN through pressure-dependent studies. *J. Phys. D Appl. Phys.* **2017**, *50*, 22LT03. [[CrossRef](#)]
28. Lamprecht, M.; Thonke, K.; Teisseyre, H.; Boćkowski, M. Extremely Slow Decay of Yellow Luminescence in Be-Doped GaN and Its Identification. *Phys. Stat. Sol. (b)* **2018**, *255*, 1800126. [[CrossRef](#)]
29. Teisseyre, H.; Boćkowski, M.; Grzegory, I.; Kozanecki, A.; Damilano, B.; Zhydachevskii, Y.; Kunzer, M.; Holc, K.; Schwarz, U.T. An effective light converter for white light emitting diodes. *Appl. Phys. Lett.* **2013**, *103*, 011107. [[CrossRef](#)]
30. Grzegory, I.; Boćkowski, M.; Porowski, S. *Bulk Crystal Growth of Electronic, Optical and Optoelectronic Materials*; Capper, P., Ed.; Wiley & Sons: Hoboken, NJ, USA, 2005; p. 173.
31. Suski, T.; Litwin-Staszewska, E.; Perlin, P.; Wisniewski, P.; Teisseyre, H.; Grzegory, I.; Boćkowski, M.; Porowski, S.; Saarinen, K.; Nissilä, J. Optical and electrical properties of Be doped GaN bulk crystals. *J. Crystal Growth* **2001**, *230*, 368–371. [[CrossRef](#)]

32. Tuomisto, F.; Prozheeva, V.; Makkonen, I.; Myers, T.H.; Boćkowski, M.; Teisseyre, H. Amphoteric Be in GaN: Experimental Evidence for Switching between Substitutional and Interstitial Lattice Sites. *Phys. Rev. Lett.* **2017**, *119*, 196404. [[CrossRef](#)]
33. Glaser, E.R.; Freitas, J.A., Jr.; Storm, D.F.; Teisseyre, H.; Boćkowski, M. Optical and magnetic resonance studies of Be-doped GaN bulk crystals. *J. Crystal Growth* **2014**, *403*, 119–123. [[CrossRef](#)]
34. Clerjaud, B.; Côte, D.; Naud, C.; Bouanani-Rahbi, R.; Wasik, D.; Pakula, K.; Baranowski, J.M.; Suski, T.; Litwin-Staszewska, E.; Boćkowski, M.; et al. The role of oxygen and hydrogen in GaN. *Phys. B* **2001**, *308–310*, 117–121. [[CrossRef](#)]
35. Willoughby, W.R.; Zvanut, M.E.; Dashdorj, J.; Boćkowski, M. A model for Be-related photo-absorption in compensated GaN:Be substrates. *J. Appl. Phys.* **2016**, *120*, 115701. [[CrossRef](#)]
36. Willoughby, W.R.; Zvanut, M.E.; Boćkowski, M. Photo-EPR study of compensated defects in Be-doped GaN substrates. *J. Appl. Phys.* **2019**, *125*, 075701. [[CrossRef](#)]
37. Reshchikov, M.A.; Demchenko, D.O.; McNamara, J.D.; Fernández-Garrido, S.; Calarco, R. Green luminescence in Mg-doped GaN. *Phys. Rev. B* **2014**, *90*, 035207. [[CrossRef](#)]
38. Reshchikov, M.A.; Kvasov, A.A.; Bishop, M.F.; McMullen, T.; Usikov, A.; Soukhoveev, V.; Dmitriev, V.A. Tunable and abrupt thermal quenching of photoluminescence in high-resistivity Zn-doped GaN. *Phys. Rev. B* **2011**, *84*, 075212. [[CrossRef](#)]
39. Levanyuk, A.P.; Osipov, V.V. Edge luminescence of direct-gap semiconductors. *Sov. Phys. Usp.* **1981**, *24*, 187–215. [[CrossRef](#)]
40. Reshchikov, M.A.; Albarakati, N.M.; Monavarian, M.; Avrutin, V.; Morkoç, H. Thermal quenching of the yellow luminescence in GaN. *J. Appl. Phys.* **2018**, *123*, 161520. [[CrossRef](#)]
41. Reshchikov, M.A.; Demchenko, D.O.; Vorobiov, M.; Andrieiev, O.; McEwen, B.; Shahedipour-Sandvik, F.; Sierakowski, K.; Jaroszynski, P.; Boćkowski, M. Photoluminescence related to Ca in GaN. *Phys. Rev. B* **2022**, *106*, 035206. [[CrossRef](#)]
42. Reshchikov, M.A. Giant shifts of photoluminescence bands in GaN. *J. Appl. Phys.* **2020**, *127*, 055701. [[CrossRef](#)]
43. Heyd, J.; Scuseria, G.E.; Ernzerhof, M. Hybrid functionals based on a screened Coulomb potential. *J. Chem. Phys.* **2003**, *118*, 8207–8215. [[CrossRef](#)]
44. Lyons, J.L.; Janotti, A.; Van de Walle, C.G. Impact of Group-II Acceptors on the Electrical and Optical Properties of GaN. *Jpn. J. Appl. Phys.* **2013**, *52*, 08JJ04. [[CrossRef](#)]
45. Cai, X.; Yang, J.; Zhang, P.; Wei, S.-H. Origin of Deep Be Acceptor Levels in Nitride Semiconductors: The Roles of Chemical and Strain Effects. *Phys. Rev. Appl.* **2019**, *11*, 034019. [[CrossRef](#)]

Disclaimer/Publisher’s Note: The statements, opinions and data contained in all publications are solely those of the individual author(s) and contributor(s) and not of MDPI and/or the editor(s). MDPI and/or the editor(s) disclaim responsibility for any injury to people or property resulting from any ideas, methods, instructions or products referred to in the content.